ELSEVIER

International Journal of Mass Spectrometry 197 (2000) 95–103

International Journal of Mass Spectrometry

Some reactions and thermochemistry of NbO_3^-: oxidation and reduction, hydrogen bond strength, and catalytic activation of primary alcohols

P. Jackson*, K.J. Fisher, G.D. Willett

Department of Physical Chemistry, University of New South Wales, P.O. Box 1, Sydney, 2052, NSW, Australia

Received 23 July 1999; accepted 3 September 1999

Abstract

Some reactions of the Nb(V) anion NbO_3^- have been studied in the gas phase using Fourier transform ion cyclotron resonance mass spectrometry. In most instances, this ion behaves as a closed shell species, however, reactions where both the ion and neutral products were radicals were also observed. In these cases, the niobium was invariably reduced to a lower oxidation state. A value for the NbO_3^-–H bond strength is proposed, based on the observed reactivity: $D(NbO_3^-–H) = 103 \pm 9$ kcal mol^{-1}. The reactions of NbO_3^- with methanol and ethanol were also studied due to their relevance in catalytic processes. For the NbO_3^-/CH_3OH couple, the favoured pathway involves reduction of the parent ion to $NbO_3H_2^-$, dihydroxyniobium(III) oxide, and concomitant liberation of formaldehyde in a single step dehydrogenation reaction. The dehydration pathway, which liberates the neutral H_2O, competes less efficiently with the oxidation/reduction pathway. The primary product $NbO_3H_2^-$ does not appear to react with methanol. In contrast, the dehydration pathway is kinetically favoured for ethanol, with liberation of neutral ethene and formation of $NbO_4H_2^-$ observed. This reaction is extremely inefficient ($k_{exp}/k_{ADO} = 0.02$). The primary hydration product reacts even less efficiently with ethanol, in a two step process, ultimately resulting in formation of $NbO_4C_2H_6^-$. Radio-frequency acceleration of $NbO_4H_2^-$ results in regeneration of the parent ion. Overall, the results are in agreement with the hypothesis that higher order Nb–O bonds are the catalytically active centres on Nb–O surfaces. (Int J Mass Spectrom 197 (2000) 95–103) © 2000 Elsevier Science B.V.

Keywords: Metal oxide anions; Catalysis; Ion–molecule reactions; FTICR-MS

1. Introduction

Although niobium has a lower terrestrial abundance than its lighter congener vanadium, and has no analogous biochemical significance, it is of considerable commercial interest due to both catalytic [1] and superconducting [2] properties of reduced- and doped-Nb_2O_5 crystalline phases. It is widely accepted that higher order niobium–oxygen bonds are principally responsible for the catalytic activity of the solid state oxides [3]. In order to investigate this property further at a molecular level, we have used laser ablation to generate NbO_3^-, one of the smallest molecular subunits of solid Nb_2O_5. This method has been successfully utilised in the past to generate a variety of interesting cluster ions from involatile solids

* Corresponding author. E-mail: phil.jackson@www.chem.tu-berlin.de

PII S1387-3806(99)00210-9

[4–6]. The conditions under which the ions are generated are not dissimilar to those maintained during the chemical vapour deposition of thin films.

To date, there have been only a few studies of gas-phase metal oxide species containing more than one metal atom, and even fewer studies of gas phase metal oxide anions (for a review of gas phase metal anion chemistry, see [7]; for more specific articles consult [8–21]). In this article, we report experimental results for the reactions of NbO_3^- with a number of small molecules. Local density functional theory has also been used to model the ground state of this ion and calculate some thermochemical information. It is hoped that this work will shed some light on the role of both saturated Nb(V) centres and Nb–O double bonds in specific bond activations, and provide complementary information to published extended x-ray absorption fine structure (EXAFS) [22] and electron paramagnetic resonance (EPR) [23] results.

2. Experimental

The details of the direct laser vaporization (DLV)-FTMS experiment used is described elsewhere [24]. The mechanisms of anion formation under these conditions are currently being investigated [25], and results suggest that molecular species, for which electron affinity (EA) > 0, undergo resonant capture of photoejected electrons that are trapped by the ion cyclotron resonance (ICR) fields. Some experimental details are as follows: small amounts of solid Nb_2O_5 (Aldrich) were pressed into small disks inside the cavity of a stainless steel probe tip, which was subsequently attached to a stainless steel satellite and inserted into the ultrahigh vacuum (UHV) chamber of the Fourier transform ICR mass spectrometry (FTICR-MS) using a solid insertion probe. A background pressure of approximately 10^{-9} mbar was maintained using a 330 L/s turbo molecular pump backed by a three phase rotary pump. A cylindrical ICR cell (60 mm length by 30 mm radius) with electrostatic trapping plates at either end, was positioned in the bore of a 4.7 T superconducting magnet. The sample was positioned (using the insertion arm) flush in the centre of the trapping plate furthest from the laser. A Spectra Physics Nd-YAG laser operating at 1064 nm in the Q-switch mode (230 μs pulse), with a spot size focused to 0.3 mm diameter, was used to generate the ions from the solid. Reagent gases were leaked in through a heated gas inlet system to pressures of approximately 1.0×10^{-7} mbar. Cluster structures were probed via ion–molecule reaction studies using a series of oxygen-containing molecules (N_2O, CH_3OH, and CH_3CH_2OH) and a sulfur-containing molecule (H_2S). Pressure correction factors of 1.5 for N_2O, 2.1 for H_2S, 1.8 for CH_3OH, and 3.6 for CH_3CH_2OH [26], were used in the calculation of accurate reactant gas pressures for determination of second order rate constants. Some average dipole orientation (ADO) rate constants [27,28] were calculated where appropriate electric properties of the neutral molecule were available, for the determination of reaction efficiencies. The c constants, which represent the degree of dipole locking in the ion field, were set to 0.08, 0.24, and 0.20 for N_2O, CH_3OH, and H_2S, respectively. The dipole moments and polarisability volumes used in ADO calculations for N_2O, CH_3OH, and H_2S were 0.18 D, 1.71 D, and 0.97 D and 3.00 Å^3, 3.23 Å^3, and 3.66 Å^3 respectively [29,30].

The structure of $^1A_1$ (C_{3v}) NbO_3^- was investigated using the local spin density approximation (LSDA) as implemented in DMOL version 2.3.1 [31]. This implementation utilises a mixture of local exchange and correlation as defined by the von Barth/Hedin [32] and Hedin/Lundqvist functionals [33]. A double numerical basis set of 6-31G* quality was used, with the frozen core approximation applied to the $1s^2$–$3d^{10}$ electrons of Nb, and the $1s^2$ electrons of O. The thermochemical information provided at this level of theory can certainly be used as upper bounds for bond strengths and electron affinities. Moreover, the structure obtained from a calculation of this type should be of a reasonable quality, as NbO_3^- possesses 12 e^- and the closed shell configuration should be the dominant contributor to the ground-state wave function.

3. Results

At relatively low laser powers (0.5 MW cm^{-2}) it was possible to generate useful quantities of the anion of interest. At higher laser powers the overall yield of NbO_3^- decreased with respect to higher mass anion clusters, which will be the subject of a future report [34]. This result alone suggests $NbO_3^{\cdot}$ is probably produced via a direct desorption mechanism as (NbO_3) groups are prevalent on the oxide surface. This radical then recombines with a trapped photoejected electron in the ICR cell to yield NbO_3^-.

Before we begin to discuss the ion–molecule chemistry, it is pertinent to present the computational results for NbO_3^-. At the LSDA level of theory, the optimised Nb–O bond lengths in the C_{3v} anion are 1.800 Å, and the ∠O–Nb–O bond angles 116 °. The bond angles are close to the classical tetrahedral angle of 109 ° but are slightly larger, which could be due to a combination of O–O lone pair repulsions and the absence of a ligand in the fourth coordination position. The umbrella inversion motion requires a mere 400 cm^{-1}*, which strongly suggests the ion is floppy and incoming nucleophiles should not be significantly hindered by oxygen repulsions. The energy required to reduce NbO_3^- to NbO_2^- [formally Nb(III)], also a closed shell ion with C_{2v} symmetry,† is 184.8 kcal mol^{-1}, which seems to agree very well with the value for D(Nb–O) = 187 ± 20 kcal mol^{-1} derived from thermochemical data [35]. Before continuing, it should be noted that this energy does not take into account the fact that Nb–O bond fission from ground state NbO_3^- to ground state $^1NbO_2^-$ is spin forbidden, which may dramatically increase this bond energy,‡ hence comparisons of the computational value with ion beam results will require a cautious approach. We have also assumed that there are no extreme electronic effects accompanying successive ligation of the metal centre [36]. Nevertheless, we can assume that fission reactions involving liberation of atomic oxygen should be high energy processes and as such are uncommon, but not altogether unfeasible, under ion-molecule reaction conditions. Noting the low level of the calculations and the well known tendency of the LSDA to strengthen bonds, we adopt a value of $D(NbO_2^-–O)$ = 175 ± 10 kcal mol^{-1}.

We have also calculated the adiabatic detachment energy of NbO_3^- using LSDA, and the value obtained (94.8 kcal mol^{-1}) is rather large, but consistent with electron loss from a closed shell species with a high chalcogenide:metal ratio. We adopt the value EA(NbO_3) = 85 ± 10 kcal mol^{-1} for future reference.

The collision-induced dissociation (CID) spectrum of NbO_3^- in argon is presented in Fig. 1. The rf irradiation time was 40 μs. The delay before detection corresponds to approximately one collision. The major dissociation channel is loss of O, with a minor peak corresponding to loss of dioxygen anion. Such a fragmentation pattern is entirely consistent with the ground state of NbO_3^-, in which there is no O–O bonding. The peak at *m/z* 70.5 is an artefact of the Fourier transform process. As the irradiation time was increased beyond 40 μs, and thus the collision energy was increased, a sharp decrease in the signal to noise ratio was noted, suggesting electron detachment was efficiently competing with bond fission. Although this is also the case at lower energies, it is particularly fortunate that good ion yields were obtained from laser ablation, thereby enabling fission product detection. It is doubtful that useful collision induced dissociation results would have been obtained for lower ion concentrations.

No reactions were observed between NbO_3^- and either C_6H_6 or CO, so that $D(NbO_2^-–O) > D$(OC–O) = 127.3 kcal mol^{-1}. This result is in accord with the theoretical value for this bond strength, if we assume there are no spin barriers operative. The lack of reactivity with benzene comes as a surprise con-

* The singlet D_{3h} isomer is a transition structure according to LSDA (ω_{im} = 136*i* cm^{-1}), r_e = 1.808 Å.

† Two stationary points were located for NbO_2^-, and both were found to be minima. The lowest energy of these was a singlet with C_{2v} symmetry, r(Nb–O) = 1.750 Å, ∠O–Nb–O = 104.3°, and self-consistent field (SCF) binding energy of 417.3 kcal mol^{-1}, zero point energy of 3.2 kcal mol^{-1}. The first triplet state resides a mere 4.9 kcal mol^{-1} above the singlet state, r(Nb–O) = 1.777 Å, ∠O–Nb–O = 113.7°, SCF binding energy = 412.3 kcal mol^{-1}, zero point energy = 3.0 kcal mol^{-1}.

‡ According to our calculations, $\Delta H_{r,0}(^1NbO_3^- \rightarrow {}^3NbO_2^- + {}^3O)$ = 190.0 kcal mol^{-1}, which is not a considerable increase in endothermicity.

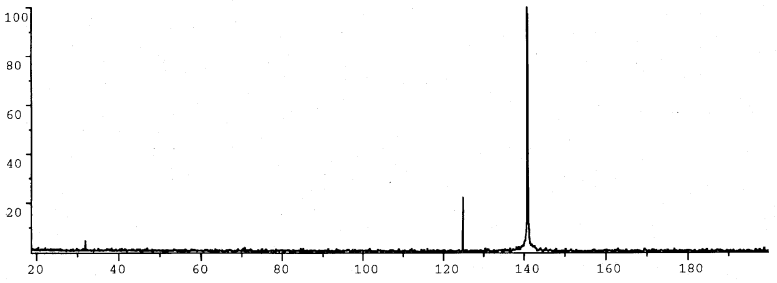

Fig. 1. Collision induced dissociation spectrum of NbO_3^- after approximately one collision, using argon as the collision gas. The rf-irradiation time is 40 μs. The peak nearest the parent ion corresponds to loss of O.

sidering the fourth coordination position is available. Moreover, theoretical studies of VO_3^- [16] suggest that NbO_3^- should be an extremely polar ion with a charge-depleted metal centre. While oxygen transfer from NbO_3^- to C_6H_6, forming C_6H_5OH is clearly endothermic, hydrogen transfer should be slightly exothermic according to the reaction between NbO_3^- and H_2O (vide infra). The reason no reaction is observed with C_6H_6 is probably steric, and detailed theoretical investigations are required to establish this.

It is appropriate to begin discussion with the simplest couples, that is, NbO_3^- with H_2O and N_2O. The reasoning for this is twofold: first, any thermochemical results established can be used to rationalise reactions observed for more complex ion–neutral couples, and second, the neutral energetics for H_2O and N_2O are well-defined.

After isolating NbO_3^-, it was allowed to undergo reactions with H_2O that is ubiquitous in the ICR cell, even at 2–5 $\times$ 10^{-9} mbar pressure. No absolute rate constants are reported, as there are no means of measuring an accurate pressure of H_2O under these circumstances, although it is certainly less than 2 $\times$ 10^{-9} mbar. For this reason, the overall reaction is slow (the collision frequency is approximately 0.1–0.2 s^{-1}). From Fig. 2, it is apparent that two exothermic pathways compete at lab energies. The first is simple water addition, whereas the second (less efficient) pathway seemingly involves either H_2 abstraction from H_2O, or H_2O addition and O elimination. It is more probable that NbO_3^- reacts with a contaminant background gas to give rise to $NbO_3H_2^-$. Single H-abstraction products were not observed. The low pressures maintained for this experiment also preclude more complex termolecular processes taking place. Nevertheless, we cannot completely exclude the activation of both H–O bonds of water, but the lack of a C–H bond activation reaction with benzene casts some doubt over this proceeding at thermal energies.

A qualitative representation of the potential energy surface leading to the products is given in Fig. 3. The initial ion–molecule complex lies well below the first entrance channel, as there is sufficient internal energy remaining, after formation of the Nb(V) product $NbO_4H_2^-$, for Nb–O fission to take place, leaving the reduced Nb(III) product $NbO_3H_2^-$. It is assumed that this ion product is formed in the triplet state. Un-

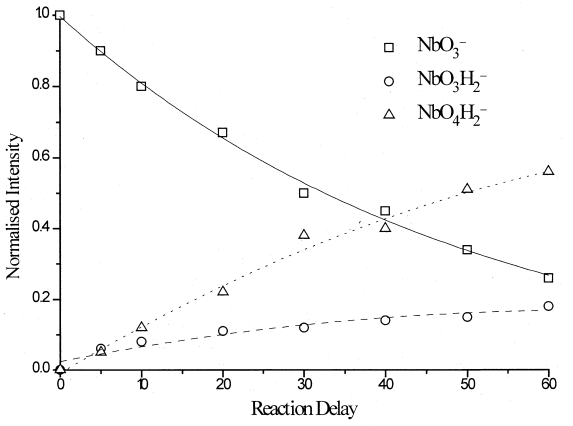

Fig. 2. Temporal profile of the reaction products for the couple NbO_3^-/H_2O detected using FTICR-MS.

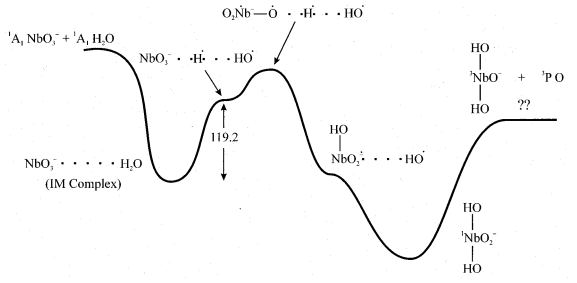

Fig. 3. Qualitative ion–molecule reaction surface for the NbO_3^-/H_2O couple, deduced from ion–molecule reaction results.

known features of the potential energy surface include the energy required for formation of the NbO_3^- radical, which necessitates Nb–O bond slippage, as well as various energies imparted to/lost from the ion–molecule complex via bond formations/fissions. We have also assumed that the barrier for coupling of $OH^{\cdot}$ and $NbO_3H^{\cdot -}$ is negligible. It is known that highly oxidised early transition metal–oxo ions are capable of activating very inert molecules [37].

The reaction with N_2O is very inefficient, and after a reaction delay of 10 s at a corrected pressure of 6.7×10^{-8} mbar, two products are observed, NbO_4^- and NbO_5^-, corresponding to sequential oxygen transfer reactions from N_2O. After 10 s approximately 95% of the parent ion was left, so that $k_{expt} < 7.1 \times 10^{-11}$ cm^3 $molecule^{-1}$ s^{-1}. Due to the method of ion formation, the small fraction of ions that have reacted are probably vibrationally/kinetically excited, and the reaction from the ground vibrational state is hindered. The barrier could be due to either the low polarisability of N_2O, or formation of a high-spin hypervalent ion product (NbO_4^-), which in any case would be spin forbidden. NbO_4^- then rapidly reacts to add a further oxygen atom, probably leading to formation of an electrostatic $[O_3Nb–O_2]^-$ complex. From this result, $D(O_3Nb^-–O) < D(N_2O) = 40$ kcal mol^{-1}.

A convenient route to the synthesis of metal sulfide clusters or ions in the gas phase is through conversion of the analogous oxide ion by reaction with COS or H_2S [38]. Organic thiols can also be used if the vapour pressure is suitably high. Although $D(O_yM_x–O)$ is usually stronger than $D(O_yM_x–S)$, the reaction is driven by the high thermochemical stability of the neutral that is formed, which for thiols is H_2O, and in the case of COS, CO_2. For a reaction to take place under ICR conditions with H_2S as the reactive neutral $D(O_yM_x–O) - D(O_yM_x–S) < 52.9$ kcal mol^{-1}, and COS as the reactive neutral $D(O_yM_x–O) - D(O_yM_x–S) < 60.1$ kcal mol^{-1}.

The major reaction products for the NbO_3^-/H_2S couple are NbO_3H^-, HS^-, and NbO_2S^-. The sulfur–oxygen substitution process was observed to proceed until all of the oxygen atoms of the parent ion were replaced, and the ions NbO_2S^-, $NbOS_2^-$, and NbS_3^- were all detected as reaction products at longer reaction delays. The branching ratio is

$$NbO_3^- + H_2S \xrightarrow{1\ \text{collision}} \begin{cases} NbO_3H^{\cdot -} + HS^{\cdot} & 10\% \\ NbO_2S^- + H_2O & 40\% \\ HS^- + NbO_3H & 50\% \end{cases}$$

The rate of disappearance of NbO_3^- was determined to be 1.8×10^{-10} cm^3 $molecule^{-1}$ s^{-1}, from which a reaction efficiency (k_{exp}/k_{ADO}) of 0.15 was calculated. This low efficiency is comparable to the rate of reaction with H_2O (vide supra), and the slow rate is attributable to the first hydrogen bond activation step. We envisage no spin barriers in the S–O substitution process, as both ligands prefer divalency and formation of M–S double bonds should be facile for a high valent transition metal such as niobium. In addition, there appear to be no spin barriers for any of the reactions of NbO_3^- with H_2S that yield the ion products listed above. From these results we conclude that $D(NbO_3^-–H) > D(HS–H) = 90.3$ kcal mol^{-1} [39]. Assuming that the reaction with H_2O is also exothermic, then $D(NbO_3^-–H) = 105 \pm 15$ kcal mol^{-1} [39]. Considering there was no reaction with benzene, which implies $D(C_6H_5–H) = 110.9$ kcal

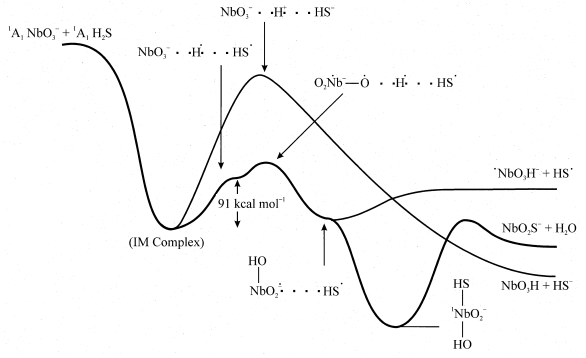

Fig. 4. Qualitative ion–molecule reaction surface for the NbO_3^-/H_2S couple, deduced from ion–molecule reaction results.

mol^{-1} > $D(NbO_3^-–H)$ [40,41], then the hydrogen bond strength value can be further refined to 101 ± 10 kcal mol^{-1}. Moreover, observation of HS^- as an exothermic reaction product infers $\Delta H_{acid}(NbO_3^-) > \Delta H_{acid}(HS^-) = 350 \pm 1$ kcal mol^{-1} [42]. A qualitative potential energy surface for the NbO_3^-/H_2S reaction is presented in Fig. 4.

More interesting than the S–O substitution products were the minor reaction products, which include NbO_2SH^-, $NbOS_2H_{1,2}^-$, and $NbS_3H_2^-$. The first of these reduction products is formally a Nb(IV) anion, as is $NbOS_2H^-$, whereas the other ions possess reduced Nb(III) centres. Numerous oxide and sulfide polymorphs have been characterised for niobium in the condensed phase, although the lower oxidation states of this metal are not as common as for vanadium.

The ion–molecule couples NbO_3^-/CH_3OH and NbO_3^-/C_2H_5OH have also been studied, and from a catalytic perspective, warrant close scrutiny. NbO_3^- reacts exothermically with CH_3OH to yield two products (Fig. 5). The kinetically favoured pathway is a formal oxidation/reduction process which liberates CH_2O as the neutral product. The hydrogen abstractions are concerted, as no peak corresponding to NbO_3H^- was detected, even after a reaction delay allowing for only one collision. The other pathway involves net methylene (CH_2) transfer to NbO_3^- and concomitant H_2O liberation. The structure of the $NbO_3CH_2^-$ product ion is assumed to possess an intact CH_2O unit, given the oxophilicity of carbon. Unfortunately, the low yields of this ion precluded isolation and CID studies, which might have been useful in determining whether the structure was an ion–dipole complex involving the closed-shell Nb(III) species NbO_2^-. Several endothermic oxygen transfer products were also detected (NbO_2^-, NbO_2H^-, and $NbO_2H_2^-$), but the intensities of these ions were very weak. The ion $NbO_2H_2^-$ is interesting, particularly if formation occurs in one collision, as this could represent a by-product in the generation of formic acid over Nb–O surfaces at slightly elevated temperatures. The primary product ion $NbO_3H_2^-$ reacts very inefficiently with CH_3OH, if at all. The endothermic oxygen transfer reaction yielding NbO_4^- and CH_4 is extremely inefficient.

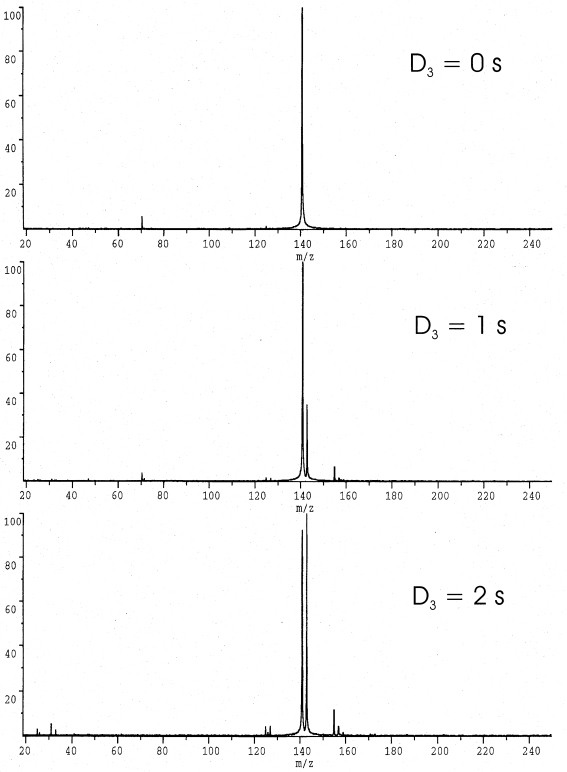

Fig. 5. Representative FTICR mass spectra for the reaction between NbO_3^- and CH_3OH for different reaction times (given on each spectrum). The major reaction products are $NbO_3H_2^-$ (*m/z* 142.8) and $NbO_3CH_2^-$ (*m/z* 154.8). See text for a more detailed discussion of the products. The peak at *m/z* 70.4 is an artefact of Fourier transform processing.

The primary reaction occurs with an ADO efficiency of 0.45 ($k_{expt} = 6.9 \times 10^{-10}$ cm^3 molecule^{-1} s^{-1}). Given the rather high efficiency of the oxidation reaction, we assume that the product ion is a reduced, closed-shell species, as formation of a triplet dihydroxyniobium(III)oxide anion would be associated with a spin barrier. If the reaction producing $NbO_3H_2^-$ is a concerted process, as the ion–molecule results suggest, it is appealing to suggest that $D(NbO_3^-–H) > D(CH_3O–H) = 104.0 \pm 0.8$ kcal mol^{-1} [40,41] which leads to $D(NbO_3^-–H) = 107 \pm 4$ kcal mol^{-1}, based on the energy required to abstract the hydroxyl hydrogen from CH_3OH. We prefer to adopt the value 103 ± 9 kcal mol^{-1} without computational knowledge of the reaction mechanism.

The reaction between C_2H_5OH and NbO_3^- is significantly slower ($k_{expt} = 2.7 \times 10^{-13}$ cm^3 molecule^{-1} s^{-1}). This corresponds to an ADO efficiency of just 0.02. Two exothermic pathways are observed; the kinetically favoured product corresponds to dehydration and neutral C_2H_4 liberation. Oxidation of C_2H_5OH to C_2H_4O is the other exothermic product. For C_2H_5OH, small amounts of the primary hydride abstraction product NbO_3H^- are also observed, so it is possible that consecutive step-wise dehydrogenation events contribute to formation of $NbO_3H_2^-$. Considering the C–H and O–H bond strengths of both methanol and ethanol, and the kinetic evolution of the product ions for the ethanol reaction, it is quite likely that concerted (2H) dehydrogenations also lead to formation of $NbO_3H_2^-$. No ion to neutral oxygen transfer products were observed at all for the reaction with C_2H_5OH, however trace amounts of $NbO_3H_3^-$ were detected, which is probably a trihydroxyniobium(II) anion. Swept ejection was used to isolate the primary ion hydration product, which was then left to react with C_2H_5OH. Three products were observed, although two of these are either reactive intermediates or endothermic products. The principle reaction product corresponds to either a substitution reaction in which H_2O is replaced by C_2H_5OH; or alternately, further dehydration liberates the neutral H_2O with C_2H_4 remaining bound to the anion. The observation of very small peaks corresponding to addition of 12 mass units ($NbO_4H_2C^-$) and addition of 2 mass units

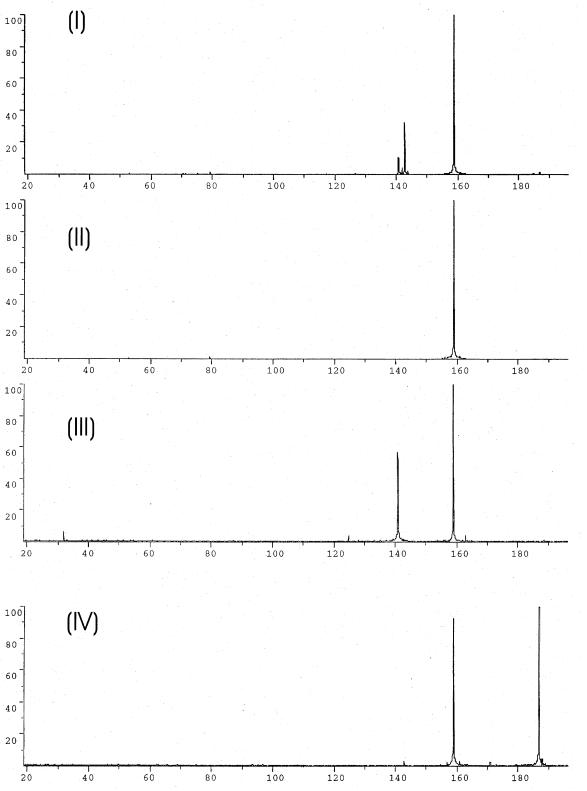

Fig. 6. (I) Representative FTICR mass spectrum for the reaction between NbO_3^- and CH_3CH_2OH after 16 s reaction delay. (II) Isolation of the major reaction product, $NbO_4H_2^-$ (*m/z* 158.8), using swept ejection. (III) rf acceleration of isolated $NbO_4H_2^-$ in the presence of the reagent gas, simulating ion heating. This results in recovery of the parent ion. (IV) Reaction of isolated $NbO_4H_2^-$ with CH_3CH_2OH after a reaction delay of 540 s. The major product corresponds to addition of *m/z* 28. Note the minor peak at *m/z* 170.8. See the text for discussion.

($NbO_4H_4^-$) gives some insight into C_2H_5OH activation by $NbO_4H_2^-$. The observation of both products suggests the primary hydration product is indeed capable of alcohol activation, and the methylene abstraction product disfavours a $H_2O–C_2H_5OH$ substitution pathway for $NbO_4H_2^-$. Thus, two neutral molecules would appear to be liberated (either H_2O and CH_4, or $CH_3OH + H_2$, the former pair being more thermochemically favourable) in the first alcohol activation, and this product ion then reacts rapidly to abstract a further CH_2 unit from C_2H_5OH, resulting in liberation of the neutral CH_3OH. This reaction is nearly two orders of magnitude slower than the first

C_2H_5OH activation by NbO_3^-, even though the hydrated product can also be envisaged as a Nb(V) species. The inefficiency of C_2H_5OH activation by the primary hydration product lends support to the hypothesis that higher-order Nb–O bonds are responsible for the catalytic activity on niobium oxide surfaces, and there are notable similarities in the reactions observed for the Nb(V) ions NbO_3^- and $NbO_4H_2^-$. In contrast, $NbO_3H_2^-$, the Nb(III)-product ion, is far less reactive toward alcohols.

In order to establish catalytic activity of NbO_3^-, swept ejection was again used to isolate the primary hydration product, which was then accelerated using a single rf pulse, of 40 μs duration, in the presence of C_2H_5OH. This experiment resulted in regeneration of NbO_3^- plus small amounts of O_2^- and NbO_2^- (Fig. 6). Thus, we have mimicked dehydration of poisoned catalyst surfaces by heating. It is hoped that future labelling experiments and theoretical studies might assist in the determination of reaction mechanisms.

Acknowledgements

One of the authors (P.J.) would like to thank the Nuclear Medicine Research Foundation (Dr. Hans Van der Wall) and the Australian Nuclear Science and Technology Organisation for financial assistance through the course of his doctoral studies. The remaining authors (K.J.F. and G.D.W.) gratefully acknowledge the assistance of the Australian Research Council. Insightful discussions with Sejin Jeong (UNSW) and Dr. Ilona Kretzschmar (Technical University, Berlin) are appreciated. The authors also thank Professor I. G. Dance for access to the DMOL computing package.

References

[1] I.E. Wachs, Proceedings of the International Conference on Niobium and Tantalum, 1989, p. 679.
[2] D.L. Novikov, V.A. Gubanov, A.J. Freeman, S.A. Turzhevsky, Phys. Rev. B 50 (1994) 3200.
[3] J.M. Jehng, I.E. Wachs, Catal. Today 8 (1990) 37.
[4] J. El-Nakat, I.G. Dance, K.J. Fisher, G.D. Willett, J. Chem. Soc. Chem. Commun. (1991) 746.
[5] J. El-Nakat, I.G. Dance, K.J. Fisher, G.D. Willett, Inorg. Chem. 32 (1993) 1931.
[6] P. Jackson, G.E. Gadd, K.J. Fisher, I.G. Dance, G.D. Willett, Int. J. Mass Spectrom. Ion Processes 157/158 (1996) 329.
[7] R. Squires, Chem. Rev. 87 (1987) 623.
[8] J.K. Gibson, J. Phys. Chem. 98 (1994) 11321.
[9] J.K. Gibson, J. Phys. Chem. 98 (1994) 6063.
[10] C.J. Cassady, D.A. Weil, S.W. McElvany, J. Chem. Phys. 96 (1992) 691.
[11] R.G. Keesee, B. Chen, A.C. Harms, A.W. Castleman Jr., Int. J. Mass Spectrom. Ion Processes 123 (1993) 225.
[12] O. Gehret, M.P. Irion, Eur. J. Chem. 2 (1996) 598.
[13] H.T. Deng, K.P. Kerns, A.W. Castleman Jr., J. Phys. Chem. 100 (1996) 13386.
[14] C.J. Cassady, S.W. McElvany, Organometallics 11 (1992) 2367.
[15] J.M. Parnis, R.D. Lafleur, D.M. Rayner, J. Phys. Chem. 99 (1995) 673.
[16] A. Dinca, T.P. Davis, K.J. Fisher, D.R. Smith, G.D. Willett, Int. J. Mass Spectrom. Ion Processes 182/183 (1999) 73.
[17] Y. Shi, K.M. Ervin, J. Chem. Phys. 108 (1998) 1757.
[18] P. Schnabel, M.P. Irion, K.G. Weil, J. Phys. Chem. 95 (1991) 9688.
[19] M. Kinne, K. Rademann, Chem. Phys. Lett. 284 (1998) 363.
[20] M. Kinne, T.M. Bernhardt, B. Kaiser, K. Rademann, Int. J. Mass Spectrom. Ion Processes 167/168 (1997) 161.
[21] M. Kinne, T.M. Bernhardt, B. Kaiser, K. Rademann, Z. Phys. D 40 (1997) 105.
[22] Y. Wada, A. Morikawa, Catal. Today 8 (1990) 13.
[23] M. Shirai, N. Ichikumi, K. Asakura, Y. Iwasaw, Catal. Today 8 (1990) 57.
[24] P.F. Greenwood, M.A. Wilson, G.D. Willett, Org. Mass Spectrom. 28 (1993) 831.
[25] P. Jackson, Ph.D. dissertation, University of New South Wales, 1998.
[26] R.L. Summers, in NASA Technical Note no. TND-5285, Lewis Research Centre, National Aeronautics and Space Administration Centre, Washington, DC, 1969.
[27] T. Su, M.T. Bowers, J. Chem. Phys. 58 (1973) 3027.
[28] L. Bass, T. Su, W.J. Chesnavich, M.T. Bowers, Chem. Phys. Lett. 34 (1975) 119.
[29] CRC Handbook of Chemistry and Physics, R.C. Weast (Ed.), Chemical Rubber, Boca Raton, FL, 1986.
[30] Molecular Theory of Gases and Liquids, J.O. Hirschfelder, C.F. Curtiss, R. Byron Bird (Eds.), Wiley, New York, 1967.
[31] MSI, 9685 Scranton Road, San Diego, CA 92121-2777.
[32] U. von Barth, L. Hedin, J. Phys. C 5 (1972) 1629.
[33] L. Hedin, B.I. Lundqvist, J. Phys. C 4 (1971) 2064.
[34] P. Jackson, K.J. Fisher, G.D. Willett, unpublished.
[35] J.B. Pedley, E.M. Marshall, J. Phys. Chem. Ref. Data 12 (1983) 967.
[36] I. Kretzschmar, A. Fiedler, J.N. Harvey, D. Schröder, H. Schwarz, J. Phys. Chem. A 101 (1997) 6252.
[37] J.N. Harvey, M. Diefenbach, D. Schröder, H. Schwarz, Int. J. Mass Spectrom. Ion Processes 182/183 (1999) 85.

[38] J.N. Harvey, D. Schröder, H. Schwarz, Inorg. Chim. Acta 273 (1998) 111.
[39] M.W. Chase Jr., C.A. Davies, J.R. Downey Jr., D.J. Frurip, R.A. McDonald, A.N. Syverud, JANAF Thermochemical Tables, 3rd ed., J. Phys. Chem. Ref. Data 14, 185.
[40] J.B. Pedley, J. Rylance, in Computer-Analysed Thermochemical Data: Organic and Organometallic Compounds, University of Sussex Press, Brighton, UK, 1977, Vol. 1.
[41] D.F. McMillen, D.M. Golden, Annu. Rev. Phys. Chem. 33 (1982) 493.
[42] B.K. Janousek, J.I. Brauman, Phys. Rev. A 23 (1981) 1673.